Bull. Mater. Sci. (2022) 45:151
https://doi.org/10.1007/s12034-022-02726-0

Dense Y-PSZ electrolyte with high ionic conductivity prepared by spark plasma sintering

TAHEREH NAMDARI[1], ALI ARAB[1,*], MOHAMMAD HASSAN YOUSEFI[1], SOHRAB MANOUCHEHRI[1] and MOHAMMAD REZA LOGMAN ESTARKI[2]

[1]Department of Physics, Faculty of Science, Malek Ashtar University of Technology, Shahinshahr 83145-34177, Iran
[2]Department of Materials Engineering, Malek Ashtar University of Technology, Shahinshahr 83157-13115, Iran
*Author for correspondence (aa.arab@yahoo.com)

MS received 22 January 2022; accepted 8 April 2022

Abstract. In this study, yttria partially stabilized zirconia (Y-PSZ) powders have been prepared using the Pechini sol–gel method with molar ratios of 4, 6 and 8 acids citric to total moles of cations. To determine the density of samples and the measurement of ionic conductivity, the pellet of samples was produced using spark plasma sintering at different sintering temperatures. The density of the pellets was determined by the Archimedes method, which was from 92 to 99.9% compared to their theoretical density. Structural and microstructural properties of the optimal pellet were investigated using X-ray diffraction pattern (XRD), Raman spectroscopy and field-emission scanning electron microscopy (FE-SEM). XRD data and Raman spectrum analysis show that the crystalline structure is mainly cubic with a tetragonal phase. FE-SEM images show that the particle shape of powders is spherical with a likely uniform particle size distribution and the average sizes of particles are about 29 nm. The electrochemical properties of the optimal sample were measured by the electrochemical impedance spectrum. The results of ionic conductivity measurements in the range of room temperature up to 1000°C show the Y-PSZ optimal sample has conductivity higher than the other counterpart samples and is comparable to the 8YSZ conductivity. The association binding energy, the activation energy and the mobility energy of the optimum pellet have been calculated from the slope of the Arrhenius diagram.

Keywords. Y-PSZ; ion conductivity; activation energy; mobility energy; Arrhenius diagram; association binding energy.

1. Introduction

Zirconia is widely used due to its unique properties. Its mechanical properties, especially strength and hardness, along with its optical, ionic and electrical properties, make it suitable for many applications, such as coatings, solid oxide fuel cells and oxygen sensors. Pure zirconia at atmospheric pressure has three solid polymorphs with symmetric monoclinic, tetragonal and cubic structures. The monoclinic phase converts to the tetragonal phase at 1100°C, and the tetragonal phase converts to the cubic phase at 2400°C [1]. This phase change at different temperatures has limited pure zirconia ceramics. The conversion of the tetragonal phase to monoclinic causes 4–5% change in structure volume at high temperatures during cooling, leading to cracks and fractures in the structure, which creates mechanical stability and resistance to thermal shock reduction [2–5]. The cubic structure of ZrO_2 has a relatively open structure due to the presence of empty octahedral sites that can accelerate the conduction of oxide ions. It is necessary to stabilize zirconia's cubic structure at room temperature to use it as an electrolyte in oxygen sensors, which is achieved by additives such as trivalent rare-earth cations [6]. The addition of trivalent impurities to the zirconia lattice creates a defect of oxygen depletion due to maintaining the neutrality of the charges. At high temperatures, the movement of these depletions causes the delivery of oxygen ions. The concentration of depletions in moving oxygen is affected by the elastic tensile energy, which depends on the size mismatch between the host and substituent cations [6,7]. In addition, to prevent changing the cubic phase to the monoclinic phase, adding contaminants to ZrO_2 can improve the concentration of oxygen ion voids, leading to high oxygen ion conductivity at high temperatures. The electrical properties and stability of ZrO_2-based electrolytes strongly depend on the type and concentration of the contaminant [8]. Accordingly, stabilized zirconia with 8% molar yttrium has many applications in oxygen sensors and fuel cells due to its high ionic conductivity, but the mechanical properties of 4YSZ (4 mol% Y_2O_3 and 96 mol% ZrO_2) are significantly higher than 8YSZ (8 mol% Y_2O_3 and 96 mol% ZrO_2). 4YSZ is yttria partially stabilized zirconia (Y-PSZ) because its structure is not completely cubic phase and include tetragonal phase

Published online: 04 August 2022

too. However, 8YSZ is yttria completely stabilized zirconia and just has cubic phase.

For porosities above 10%, both compositions 4YSZ and 8YSZ had a significant reduction in ionic conductivity [9]. The density of the samples affects the grain boundary conduction because the grain boundary conduction depends on factors such as the effective grain boundary conduction area, the grain boundary thickness and the specific grain boundary conduction, which are mainly dependent on the microstructure and sample density [9]. There is a linear relationship between the relative density of the sample and the conductivity of the grains [10]. Various methods have been reported to prepare yttria-stabilized zirconia powders. In 1970, Pechini tested a chemical method based on polymer precursors made from acid citric and ethylene glycol. The purpose of this method is to stabilize metal ions in a rigid polymer lattice. Metal ions disperse in the polymer lattice at the atomic scale without deposition and phase separation [4]. The spark plasma sintering (SPS) method is a rapid sintering method for making ceramic samples. It can lead to homogeneous grains in a vacuum environment and bring the samples closer to their theoretical density. Higher density-stabilized zirconia ceramic specimens showed better ionic conductivity [9], but there are no reports to produce high density 4YSZ ceramic using the single-cycle sintering method.

In this research, the focus is on the fabrication of 4YSZ ceramics with high density and low porosity using SPS single-cycle methods of 4YSZ powders produced using the Pechini method and can be used for electrolytes. In addition, the structural properties, density, porosity and ionic conductivity of the samples have been studied.

2. Experimental

The raw materials used for the preparation of 4YSZ powders using the Pechini method were octa-zirconium oxychloride ($ZrOCl_2{\cdot}8H_2O$), yttrium nitrate hexahydrate ($Y(NO_3)_3{\cdot}6H_2O$), acid citric ($C_6H_8O_7$) and ethylene glycol ($(CH_2OH)_2$), all made by German Merck company with a purity of more than 99%. The powder samples were prepared with a molar ratio of 4% Y_2O_3 and 96% ZrO_2. The molar ratio 4, 6 and 8 of $C_6H_8O_7$ to Y_2O_3 and ZrO_2 were studied to achieve the higher dense ceramic. The molar ratio of $(CH_2OH)_2$ equals $C_6H_8O_7$.

At first, the cationic salts $ZrOCl_2{\cdot}8H_2O$ and $Y(NO_3)_3{\cdot}6H_2O$ with suitable molar percentages were dissolved separately in water, and then the two solutions were mixed at room temperature. While stirring the mixture, an aqueous solution of $C_6H_8O_7$ with a determined molar ratio was added and after 1-h, $(CH_2OH)_2$ was added to the mix. The resulting solution was heated at 100°C for 2 h, then left at 200°C for 2 h. The resulting jelly solution was dried in an oven at 250°C for 10 h. Finally, the dried jellies were calcined at 1000°C for 2 h. The pellets (with a diameter of 8.3 mm, and a thickness of about 2 mm) were made by the SPS method (under vacuum conditions of 10^{-3} Pa, current of 1200 A and a temperature rate of 100°C min^{-1} with uniaxial pressure of 80 MPa for 10 min) at different temperatures 1250, 1400 and 1550°C. Above 1600°C, grain growth and mechanical properties are expected to decrease, so higher temperatures were not checked in this study. At a temperature of 1550°C, the density of the sample was close to the theoretical density of 4YSZ and there was no need for higher temperatures.

A layer with an ideal metal should be placed on either sides of the optimal pellet as an electrode for checking ionic conductivity. For this purpose, platinum metal is suitable as a catalyst to show good sensitivity to oxygen in the atmosphere with which it is in contact. For electrode placement, the platinum paste was placed on the surface of the optimal pellet and then kept at 900°C for 2 h to allow the electrode to adhere well to the pellet.

The density of the pellets was calculated by Archimedes method using dry mass and wet mass measurements. X-ray diffraction pattern (XRD) of the samples was performed by XRD-Siemens-D500 with Cu-Kα radiation and wavelength of λ = 1.5406 Å. XRD was measured at room temperature in the range of 2θ between 20° and 80°. A scanning electron microscopy (FE_SEM) image was taken with MIR-A3TESCAN-XMU. Raman spectrum was obtained by laboratory arrangement with Nd:YAG laser at 537 nm. The Electrochemical impedance spectrum (EIS) of the electrode sample was taken at 1000°C using the PARSTAT2273 device in GIS mode in the frequency range of 2–100 MHz with a current of 2 μA, in 100 points.

3. Results and discussion

According to Chen *et al* [9], the optimal expected pellets must have structural porosity of less than 10% suitable for electrolyte applications. The experimental density should be close to the theoretical density, which is 6.050 g cm^{-3} for the 4YSZ sample [11]. The optimal conditions for electrolyte applications lead to the highest density. The obtained powders have been calcined at 1000°C temperature, and their pellets have been prepared at sintering 1400°C temperature. The data of samples are shown in table 1. It can be seen that the density of the sample obtained at a molarity of 8 is more significant than that of the samples obtained at molarities of 4 and 6. This density value of the sample obtained at molarity 8 is optimal. The optimized sample powders were sintered at different temperatures 1200, 1400 and 1550°C to investigate the effect of sintering temperature.

The density and porosity percentages of samples are shown in table 2. The data in table 2 indicate that the prepared pellet at 1550°C temperature has the lowest porosity and highest density. The density of this sample is 99.9% compared to those of the theory. This value is comparable

Table 1. Density and porosity percentage of the prepared pellets of powders with different molarity of acid citric (the calcined powders at 1000°C temperature and the sintered pellets at 1400°C temperature).

Molar ratio of citric acid	Density percentage	Porosity percentage
8	97.7	2.3
6	92	8
4	97	3

Table 2. Density and porosity percentage of the sintered samples with molarity 8 under different temperatures.

Sintering temperature (°C)	Density percentage	Porosity percentage
1400	97.7	2.3
1250	94	6
1550	99.9	0.1

with the density of similar samples report and even more than some. Maeland *et al* [11] examined sample 4YSZ in three-step sinter and one-step sinter methods and reached densities between 87 and 97%. Chen *et al* [9] were able to increase the density of 8YSZ to 99% by five cycles in the SPS program. Therefore, the obtained conditions with the molar ratio of acid citric 8 and the sintering temperature 1550°C for the 4YSZ sample are optimized in single-cycle SPS.

The typical XRD patterns of the prepared powder with molarity 8, its pellet prepared by usual sintering method and optimized pellet prepared by SPS are shown in figures 1, 2 and 3, respectively. Comparison of the XRD patterns of the sample powder with that for standard samples shows that the patterns of the 4YSZ powder are fully compatible with the cubic structure of the YSZ (reference card 96-210-5683). However, due to the overlap of many peaks of the tetragonal structure and the cubic structure, it cannot be said with certainty that the powder is entirely stable in the cubic phase. XRD pattern of pellet prepared by usual sintering method is shown in figure 2. As can be seen clearly, the structure has changed and it is a combination of cubic and monoclinic phases. So, the normal sintering could not preserve the cubic structure of 4YSZ. The XRD pattern of the optimized pellet prepared by SPS is shown in figure 3. Comparison patterns of figures 1 and 3 indicate that all peaks agree with others and those of the mentioned standard for the YSZ sample. The Raman analysis was used as a complementary analysis to distinguish the tetragonal phase from the cubic phase [12]. Because of the overlap of some of the peaks in XRD of these two structures, the peaks of the tetragonal phase are not distinguishable from the peaks of the cubic phase. The Raman spectrum of optimized

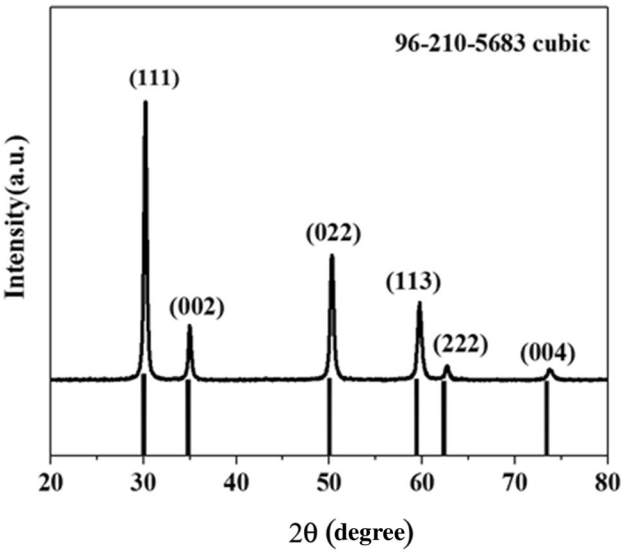

Figure 1. X-ray diffraction pattern of the prepared powder with molarity 8.

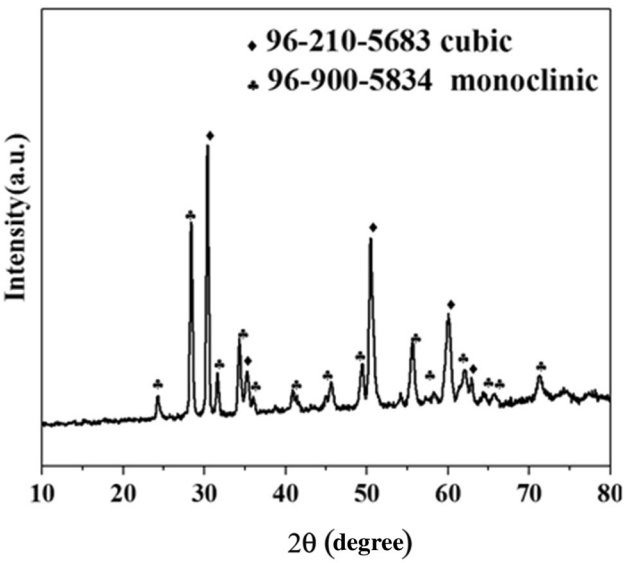

Figure 2. X-ray diffraction pattern of pellet prepared by normal sintering method.

ceramic prepared by SPS is shown in figure 4. It is seen that the peak with a wavenumber of about 1330 cm^{-1} indicates the formation of the cubic phase of the sample. Peaks in wavenumbers of about 570, 980, 1450 cm^{-1} indicate the construction of a tetragonal phase [12]. As a result, the Raman spectrum clearly shows the presence of the tetragonal phase and the cubic phase. Therefore, 4YSZ powder, due to the presence of the tetragonal phase and the cubic phase, is partially stabilized zirconia with Yttria (Y-PSZ).

The FE-SEM images of the optimum synthesized powder and its optimized pellet are shown in figure 5a and b. As shown in figure 5a, particles have around the same size

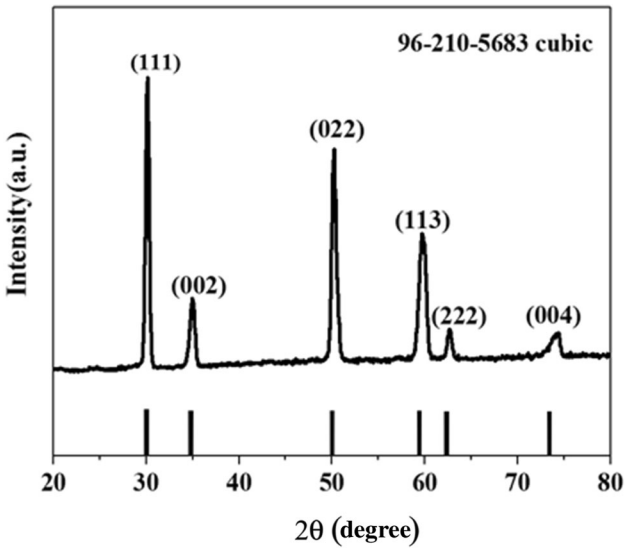

Figure 3. X-ray diffraction pattern of pellet prepared by SPS method.

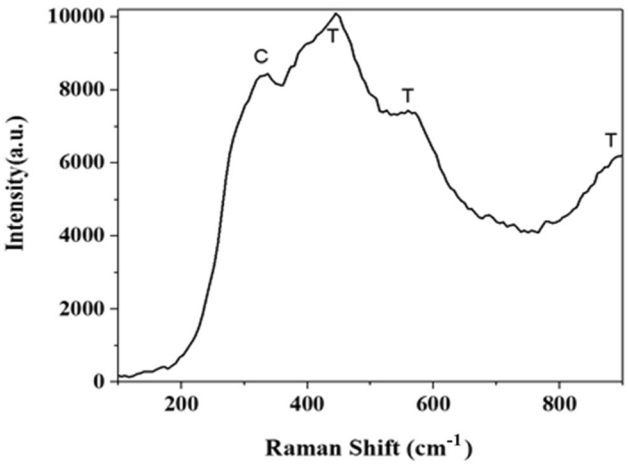

Figure 4. Raman spectrum of 4YSZ-optimized ceramics prepared by SPS method using Nd:YAG laser (wavelength 537 nm).

distribution and are spherical. The average particle size was approximately 29 nm using the Digimizer software. The microstructure of the optimized pellet Y-PSZ after sintering is illustrated in figure 5b. The images show that the particles size increases after sintering and the average particles size is about 2.5 μm. In addition, it can be seen that the porosity between particles is low, resulting in high density and large ionic conductivity.

The ionic conductivity of the optimized pellet was measured by a conductometer in the range of room temperature up to 1000°C. Its diagram variations are illustrated in figure 6. As shown in figure 6a, the conductivity of this pellet has not increased clearly up to 600°C, but it increases significantly from 600 up to 1000°C. So, the conductivity of 4YSZ ceramic has approximately reached a peak of 0.12 S cm^{-1} at 1000°C. Singhal and Kendall have reported a 4YSZ ceramic with ion conductivity of about 0.059 S cm^{-1} [13]. Arachi *et al* [14] and Feighery and Irvine [15] have stated 8YSZ ceramics with 0.14 and 0.089 S cm^{-1}, respectively. It has resulted that the ionic conductivity of the prepared 4YSZ ceramic with a density percentage of 99.9% is comparable with the ionic conductivity of 8YSZ ceramic. Because the hardness of 4YSZ ceramics is greater than 8YSZ ceramics, it is more suitable for electrolyte applications [16]. There are no reports to produce 4YSZ ceramic with high density of about 99.9% using SPS single-cycle sintering method. This lead to high ion counductivity compared to others. Some reports are compared with this study in table 3.

The activation energy can be obtained from the slope of the linear graph $\ln(\sigma T)$ in terms of $1/T$ based on the Arrhenius equation. The curve of $\ln(\sigma T)$ in terms of $1/T$ is shown in figure 6b. The slope of the curve of figure 6b at low and high temperatures is shown in figure 6c and d, respectively.

Using the slope of the linear part of the Arrhenius diagram at low temperatures (figure 6c), the mobility energy is equal to 0.078 eV (7.52585 kJ mol^{-1}). In addition, using

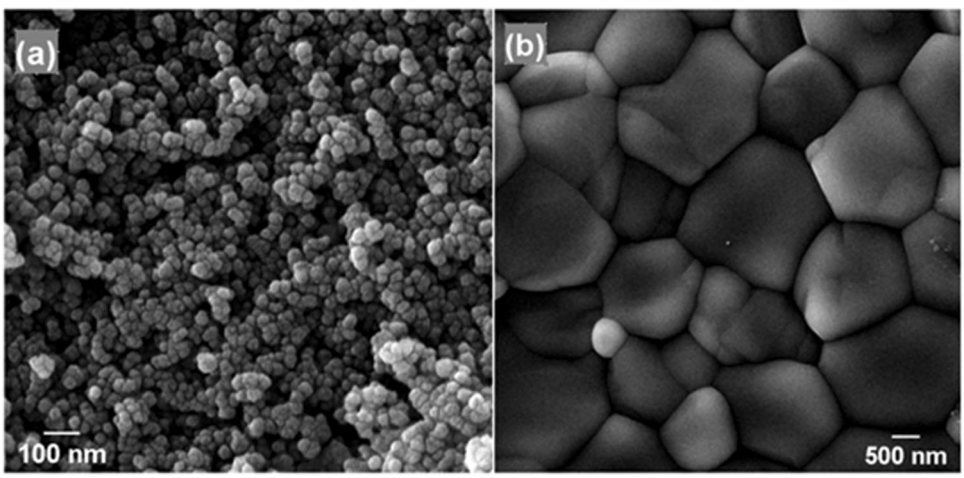

Figure 5. Scanning electron microscope image of Y-PSZ: (**a**) powder and (**b**) SPS sintered pellet.

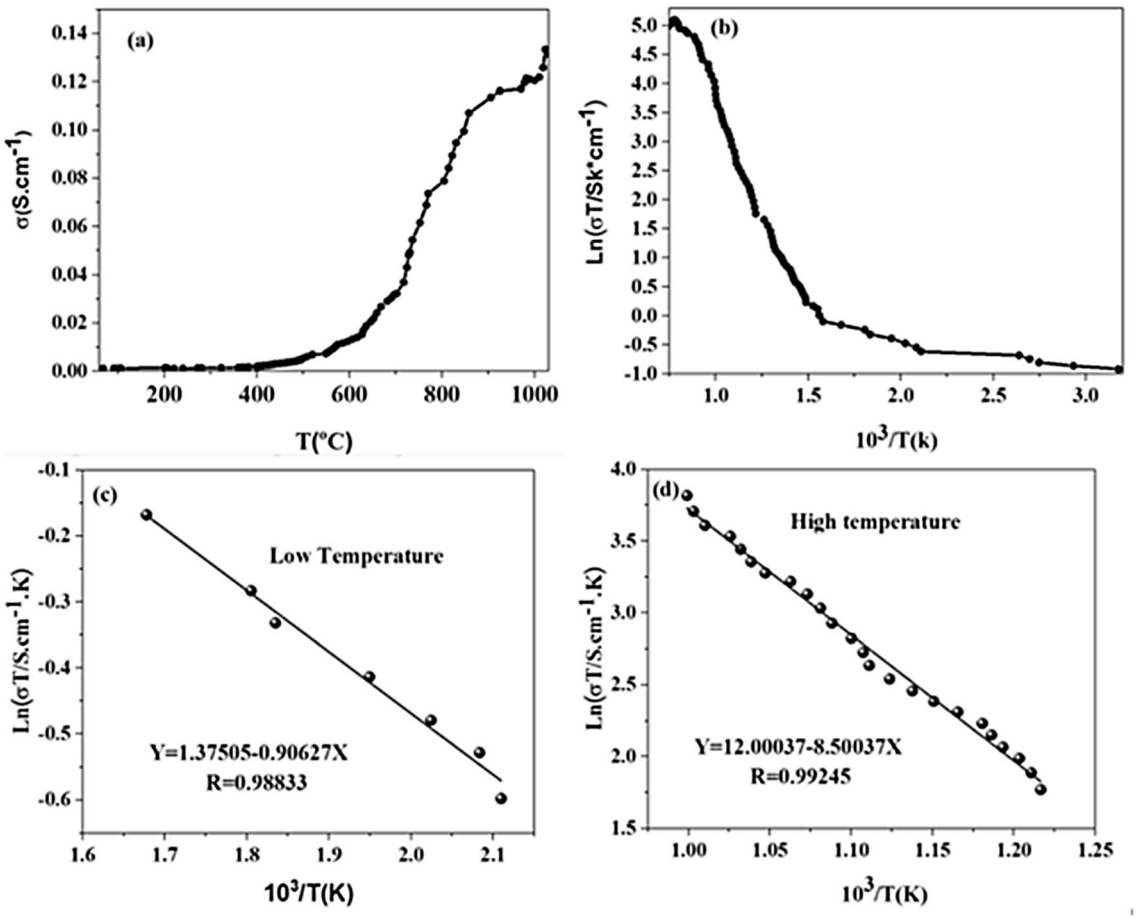

Figure 6. Optimal pellet at (**a**) temperature delivery, (**b**) Arrhenius diagram, (**c**) slope Arrhenius diagrams at (**c**) low and (**d**) high temperatures.

the slope of the linear part of the Arrhenius diagram at high temperatures (figure 6d), the activation energy was obtained, which is equal to 0.73 eV (70.434 kJ mol^{-1}). So, the difference between these two energies at high temperatures and low temperatures is comparable to 0.652 eV (62.9084 kJ mol^{-1}), named the association energy. This value is smaller than previous studies, which leads to a more significant value ion conductivity in comparison to earlier reports [19].

The Nyquist curve of the sample at 1000°C, the equivalent electrical circuit for the electrochemical impedance spectrum, the equivalent capacitance and resistance values are shown in figure 7. The solid-state electrolyte that was used, is the optimal ceramic. As can be seen, the spectrum consists of two semicircles. The first half is associated with the transfer of oxygen ions in the grain and the second half is related to the transfer of oxygen ions in the grain boundary. In addition, it can be seen that the grain boundary resistance is much higher than the grain, so the mechanism of oxygen ion transport is more through the grain. The electrical circuit equivalent to oxygen ion transport is shown in figure 6. R_2 is the grain resistance, C_2 is the grain capacitance, R_1 is the grain boundary resistance, C_1 is the grain boundary capacitance and R_3 is the residual resistance. This circuit equation is performed using ZSim software, and the values of resistors and capacitors are specified as

Table 3. Comparison of some previous studies with this work.

xYSZ	Sintering method	Temperature (°C)	Density (%)	Ion conductivity (S cm^{-1})	Reference
4YSZ	Common sintering	1200	96	3.26×10^{-6}	[17]
4YSZ	Common sintering	1300	88	—	[18]
4YSZ	Pressure-less sintering	1200	97.2	—	[19]
4YSZ	Two steps sintering	1250	97	0.0881	[20]
4YSZ	Single-cycle SPS	1550	99.9	0.12	This study

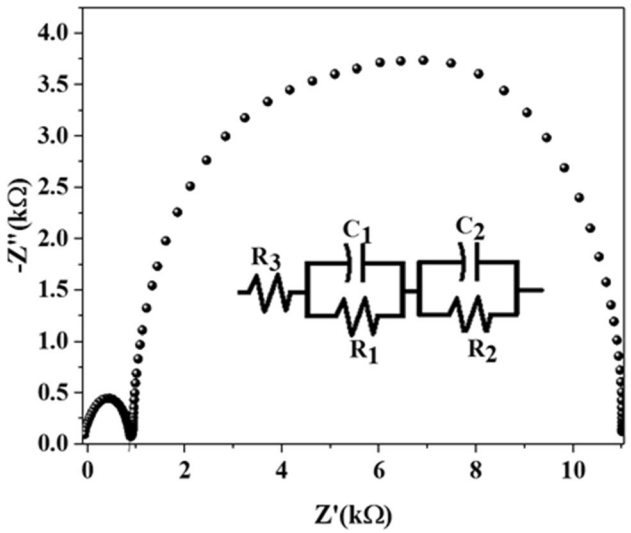

Figure 7. Electrochemical impedance spectrum (EIS) analysis of a platinum-electrode sample at 1000°C, and equivalent electrical circuit for EIS.

$R_1 = 10000\ \Omega$, $R_2 = 997\ \Omega$, $R_3 = -67\ \Omega$, $C_1 = 0.3 \times 10^{-7}$ F and $C_2 = 0.15 \times 10^{-4}$ F. Negative resistance R_3 is triggered by the formation of an interface phase, which leads to a step change of the chemical potential of the electrode. Because C_2 is the capacity of layer that is formed in grain and as seen in plot figure 7, first semicircle is related to grain and clearly is smaller than second semicircle indicating higher capacity and lower resistance relative than grain boundary.

4. Conclusion

According to the experimental results, 4YSZ powders were synthesized by the sol–gel Pechini method at the optimal conditions. For preparation of dense pellets, the SPS sintering method is a suitable method for maintaining the 4YSZ phase structure because it is done with fast sintering and there is no possibility of phase change. This led to the construction of 4YSZ dense ceramic with suitable ionic conductivity properties comparable to 4YSZ reported in other studies. Ceramic prepared by SPS method under the pressure of 80 MPa and temperature of 1550°C has a very high density (99.9%) with porosity of about 0.1% in comparison of the theoretical density. The result was that the ion conductivity of the sample is comparable with the conductivity of the other studied 8YSZ sample at the same time and had excellent mechanical properties. Thus, this fully dense 4YSZ is a suitable option for use as an electrolyte.

References

[1] Zając W and Molenda J 2008 *Solid State Ion.* **179** 154
[2] Hajizadeh-Oghaz M, Razavi R S and Estarki M L 2014 *Bull. Mater. Sci.* **37** 969
[3] Mazaheri M, Valefi M, Hesabi Z R and Sadrnezhaad S 2009 *Ceram. Int.* **35** 13
[4] Oghaz M H, Razavi R S, Loghman-Estark M R and Ghasemi R 2013 *J. Nano Res.* **21** 65
[5] Gongyi G and Yuli C 1992 *J. Am. Ceram. Soc.* **75** 1294
[6] Kendall K and Kendall M (eds) 2015 *High-temperature solid oxide fuel cells for the 21st century: fundamentals, design and applications* (UK: Elsevier)
[7] He X, Zhu Y and Mo Y 2017 *Nat. Commun.* **8** 1
[8] Liu T, Zhang X, Yuan L and Yu J 2015 *Solid State Ion.* **283** 91
[9] Chen X, Khor K, Chan S and Yu L 2003 *Mater. Sci. Eng. A* **341** 43
[10] Dong Y, Yang H, Ding D, Li J, Li J and Chen I-W 2021 *Adv. Funk. Mater.* **21** 2007750
[11] Maeland D, Suciu C, Waernhus I and Hoffmann A C 2009 *J. Eur. Ceram. Soc.* **29** 2537
[12] Basahel S N, Ali T T, Mokhtar M and Narasimharao K 2015 *Nanoscale Res. Lett.* **10** 73
[13] Singhal S C and Kendall K (eds) 2003 *High-temperature solid oxide fuel cells: fundamentals, design and applications* (Japan: International Institute for Carbon-Neutral Energy Research) p 85
[14] Arachi Y, Sakai H, Yamamoto O, Takeda Y and Imanishai N 1999 *Solid State Ion.* **121** 133
[15] Feighery A and Irvine J 1999 *Solid State Ion.* **121** 209
[16] Hwang K-J, Shin M, Lee M-H, Lee H, Oh M Y and Shin T H 2019 *Ceram. Int.* **45** 9462
[17] Guo X, Zhao X, Liu and He W J 2021 *Preprint paper in researchsquare.com* https://doi.org/10.21203/rs.3.rs-479437/v1
[18] Matsumoto M, Yamaguchi N and Matsubara H 2004 *Scr. Mater.* **50** 867
[19] Drazin J W, Wollmershauser J A, Ryou H, Wolak M A and Gorzkowski E P 2020 *J. Am. Ceram. Soc.* **103** 60
[20] Maeland D, Suciu C, Waernhus I and Hoffmann A C 2009 *J. Eur. Ceram.* **29** 2537